

# Extended-SWIR GeSn LEDs with reduced footprint and power consumption

Mahmoud R. M. Atalla<sup>†</sup>, Simone Assali, and Oussama Moutanabbir\*  
*Department of Engineering Physics, École Polytechnique de Montréal,  
C.P. 6079, Succ. Centre-Ville, Montréal, Québec, Canada H3C 3A7*

Youngmin Kim<sup>†</sup>, Daniel Burt, and Donguk Nam\*  
*School of Electrical and Electronic Engineering, Nanyang Technological University,  
50 Nanyang Avenue, Singapore 639798, Singapore. and*

<sup>†</sup>*These authors contributed equally to this work.*

CMOS-compatible short- and mid-wave infrared emitters are highly coveted for the monolithic integration of silicon-based photonic and electronic integrated circuits to serve a myriad of applications in sensing and communications. In this regard, a group IV germanium-tin (GeSn) material epitaxially grown on silicon (Si) emerges as a promising platform to implement tunable infrared light emitters. Indeed, upon increasing the Sn content, the bandgap of GeSn narrows and becomes direct, making this material system suitable for developing an efficient silicon-compatible emitter. With this perspective, microbridge PIN GeSn LEDs with a small footprint of **1,520  $\mu\text{m}^2$**  are demonstrated and their operation performance is investigated. The spectral analysis of the electroluminescence emission exhibits a peak at **2.31  $\mu\text{m}$**  and it red-shifts slightly as the driving current increases. It is found that the microbridge LED operates at a dissipated power as low as **10.8 W** at room temperature and just **3 W** at **80 K**. This demonstrated low operation power is comparable to that reported for LEDs having a significantly larger footprint reaching **10<sup>6</sup>  $\mu\text{m}^2$** . The efficient thermal dissipation of the current design helped to reduce the heat-induced optical losses, thus enhancing light emission. Further performance improvements are envisioned through thermal and optical simulations of the microbridge design. The use of GeSnOI substrate for developing a similar device is expected to improve optical confinement for the realization of electrically driven GeSn lasers.

Reducing the footprint of CMOS-compatible optical interconnects is a key paradigm to address the relentless course toward the very dense integration of chips while maintaining high bandwidth and low power consumption<sup>1-3</sup>. In fact, as future electronic chips require further device scaling, the associated miniaturization of metal interconnects suffers fundamental limits leading to high impedance and joule heating, which consequently limits the bandwidth. This stimulates a remarkable interest in merging silicon photonics with silicon-based integrated circuits for more efficient inter-chip and intra-chip communication, besides added multifunctional abilities such as on-chip optical modulation, spectroscopy, and sensing applications<sup>4</sup>. However, the development of CMOS-compatible on-chip light sources remains a huge challenge owing to the lack of direct bandgap group IV semiconductors<sup>5,6</sup>. Recently, GeSn has become a promising solution to overcome this limitation since GeSn becomes a direct bandgap material when sufficient Sn content is incorporated in Ge lattice<sup>7,8</sup>. Indeed, the indirect-direct bandgap crossover occurs at a Sn content of around 8 at. % in relaxed GeSn. Increasing the Sn content beyond this threshold improves the bandgap directness and lowers its energy, enhancing the light emission efficiency<sup>9</sup>. Photodetector devices made of chemical vapor deposition (CVD) and molecular beam epitaxy (MBE) grown layers and heterostructures have been demonstrated to operate at wavelengths up to 4.6  $\mu\text{m}$  in the mid-infrared (MIR) spectral range<sup>10</sup>. While optically pumped GeSn-based lasers have been reported by many researchers recently<sup>11</sup>, experimental attempts

to develop the electrically injected counterparts remain relatively scarce<sup>12,13</sup>.

To achieve the dense integration of Si-based integrated circuits and silicon photonics, emitters with a small footprint and reduced power consumption are strongly desired. Several efforts have been expended toward this goal<sup>14-19</sup>. While early GeSn LEDs feature low power consumption of 3.75 W, these devices have a remarkably large footprint area of around 10<sup>6</sup>  $\mu\text{m}^2$ <sup>16</sup>. Other LED devices reported later on had two orders of magnitude smaller device sizes of around 31,400  $\mu\text{m}^2$ , but they require more than 4-fold higher power consumption<sup>20</sup>. Herein, we present a GeSn microscale LED with a record-small footprint of around 1,520  $\mu\text{m}^2$  yet operating at a low dissipated power around 3 W at 80 K and around 10.8 W at room temperature. This is realized through a cavity LED utilized in a microbridge structure.

## I. RESULTS AND DISCUSSION

### Growth and characterization of GeSn epilayers and LED fabrication.

The GeSn LED samples were grown using a low-pressure CVD reactor following a multilayer growth to control lattice strain and Sn content, as schematically illustrated in Fig. 1(a). Starting from a 4-inch Si (100) wafer, a 2.67  $\mu\text{m}$  thick Ge virtual substrate (VS) was grown using 10% monogermane ( $\text{GeH}_4$ ) and a constant ultrapure

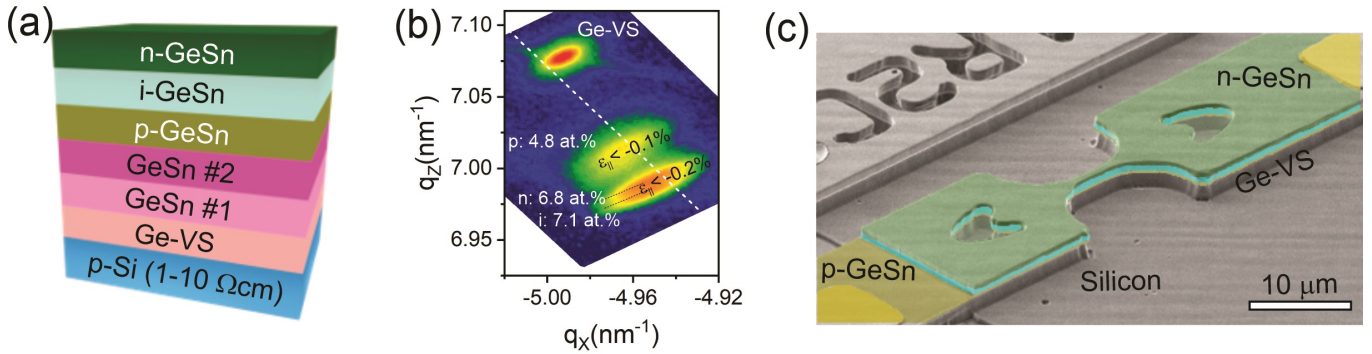


FIG. 1. (a) Schematic of the multilayer PIN GeSn growth on Si. (b) RSM measurement around the asymmetrical (224) XRD reflection peak indicating the Sn content and strain in the multilayer structure in panel (a). (c) Tilted SEM depicting the microbridge PIN GeSn LED.

H<sub>2</sub> flow implementing a two-temperature growth process at 450 and 600 °C, followed by thermal cyclic annealing above 800 °C. Two GeSn buffer layers, with thicknesses of 140 and 208 nm, were grown using GeH<sub>4</sub> and tin-tetrachloride (SnCl<sub>4</sub>) precursors at initial molar fractions of ( $1.2 \times 10^{-2}$ ) and ( $9.1 \times 10^{-6}$ ), respectively. The second GeSn buffer layer was grown at a low temperature allowing more Sn to be substitutionally incorporated into the Ge lattice. Then, PIN GeSn layers were grown at thicknesses of 375, 830, and 330 nm, respectively. The p- and n-type doping were achieved using diborane (B<sub>2</sub>H<sub>6</sub>) and arsine (AsH<sub>3</sub>) precursors, respectively. According to the X-ray diffraction (XRD) reciprocal space mapping (RSM) measured around the asymmetrical (224) reflection peak, as shown in Fig. 1(b), the Sn content is estimated to be 4.1 at. % (#1), 6 at. % (#2), 4.8 at. % (p-GeSn), 7.1 at. % (i-GeSn), 6.8 at. % (n-GeSn), respectively. It is also noticeable that the layers are remarkably relaxed with the highest bi-axial compressive strain below  $-0.2\%$  in the i- and n-GeSn layers.

Figure 1(c) displays a scanning electron microscope (SEM) image depicting the fabricated microbridge PIN GeSn LED device. The fabricated device has a microbridge structure for the diodes with a corner-cube cavity which was intended to enhance the light emission via optical confinement<sup>21</sup>. The microbridge structure with corner-cube mirrors were patterned using photolithography, and the defined pattern was transferred onto the GeSn and Ge VS layers using reactive ion etching (RIE) with Cl<sub>2</sub> chemistry. A second photolithography step was performed to anisotropically etch down to expose the p-doped GeSn layer at one end of the device. Thus, the device had exposed p- and n-doped GeSn areas on both ends of the microbridge structure. The patterns for the metal contacts were then defined using photolithography at the p- and n-doped GeSn areas. Subsequently, the Cr and Au contacts with thicknesses of 20 nm and 180 nm, respectively, were deposited as p- and n-layers using electron beam evaporation, followed by the lift-off process.

### GeSn PIN LED characterization and performance

#### comparison.

The microbridge device characterization started by measuring the I-V curves using a source meter unit over a wide bias range of up to 5 V in the forward and reverse biases as shown in Fig. 2(a). The LED operates under forward bias reaching up to 2.16 mA at 5V, which corresponds to a power consumption as low as 10.8 W at such relatively high operation bias. The large current under the reverse bias, however, indicates carrier leakage through the depletion region of the device possibly owing to various mechanisms including SRH, tunnel assisted, and diffusion leakages<sup>22-24</sup>.

To measure and analyze the LED light emission, a Fourier transform infrared spectroscopy (FTIR) setup was utilised to measure the spectral emission from the microbridge devices. The setup mainly consists of a Bruker FTIR spectrometer, InSb liquid nitrogen cooled photodetector (PD), 40× reflective objective lens, and a translation stage. To amplify the InSb PD signal, it was fed into a current preamplifier and a lock-in amplifier. The signal was re-entered into the FTIR for data processing. The lock-in technique requires the LED light to take the form of pulses either by mounting a mechanical chopper in the light path or by applying AC drive current to the LED. As shown in Fig. 2(b), the electroluminescence (EL) was measured at a driving current from 2 mA to 6 mA with 1 mA stepwise. It is evident that the LED emission peak is centered around 2.31 μm at the lowest drive current, and it red-shifts as the drive current increases, as shown in the inset of Fig. 2(b). The inset also depicts that the integrated intensity of the EL emission initially increases linearly as the driving current increases, while it saturates at 6 V, indicating the drop in the LED emission efficiency possibly due to the heating effect.

The device was also characterized at a cryogenic temperature of 80 K, showing that a clear signal can be measured at a driving current as low as 1 mA. Figure 2(c) shows the EL emission spectra measured at 80 K. It is also clear that the EL peak blue-shifts to 2.08 μm at 80

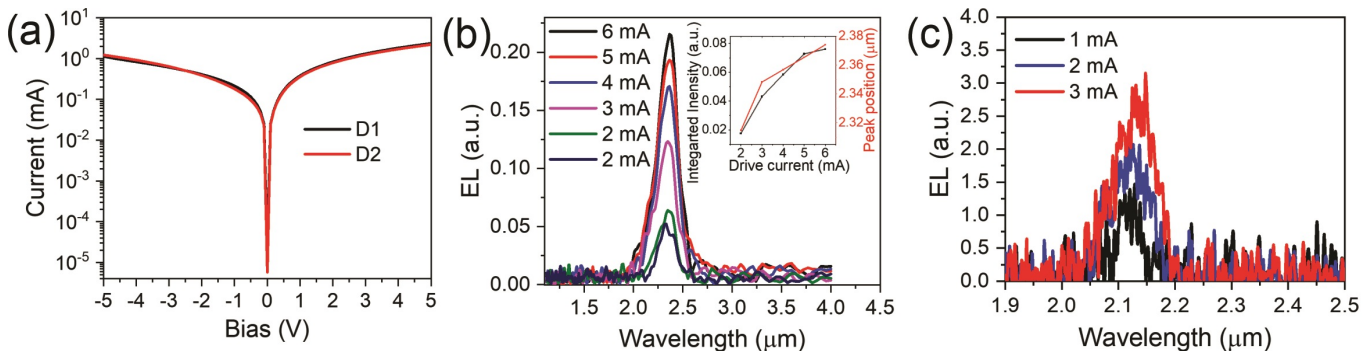


FIG. 2. (a) I-V measurement for two microbridge PIN LEDs showing the forward and reverse bias operation. (b) Electroluminescence (EL) as function of wavelength at the indicated LED drive current at room temperature. Inset: The integrated intensity and peak position as the drive current increases. (c) same as (b) but at 80 K temperature.

K compared to a significantly longer wavelength of 2.31  $\mu\text{m}$  measured at room temperature, which is attributed to the increased bandgap at a lower temperature. Table 1 compares the GeSn LEDs reported until today with a focus on comparing the dissipated power and the device footprint. The table clearly shows that our microbridge LED devices have the lowest combined footprint ( $\mu\text{m}^2$ ) and power dissipation (I-V) at room temperature and 80 K.

### Corner-cube cavity light confinement effects for improving LED emission and gain properties

To investigate why the cavity effect is not achieved in our LEDs and provide a viable pathway towards achieving cavity effects and possibly lasing, we performed thermal and optical simulations for the LED structures. Figure 3 presents simulated thermal (top) and optical fields (bottom) distributions calculated using a finite-element method (FEM) and finite-difference time-domain (FDTD), respectively, for three different LED structures. The three structures mimicked the structure used in our experiments and they consisted of: (i) the current device with no under etch (Fig. 3(a)), (ii) suspended structure with Ge VS layer under-etched except at the two ends of the device (Fig. 3(b)), and (iii) ideal fully released GeSn layer (Fig. 3(c)), which is possible by utilizing a GeSn-on-insulator (GeSnOI) structure<sup>25,26</sup>. In the thermal simulation, a heat source with a current density of  $300 \text{ Acm}^2$  was applied along the current path. The optical field distributions for the three structures were calculated at 2155 nm in the optical simulation. All the simulations were conducted at 4 K. As shown in Fig. 3(a), the LED used in our experiments shows superior thermal conduction with a slightly increased temperature of  $\sim 10$  K but it has poor optical confinement with a very low Q factor of 26 due to the significant leakage of optical fields from the GeSn active layer to the Ge VS layer underneath. This explains why the cavity effect is not observed during our experiments. To address the limited optical confinement, we designed and

investigated a structure suspended in the air that can be fabricated by etching the Ge VS layer<sup>27</sup>. In stark contrast to poor optical confinement in the structure used in our experiments, a suspended structure, as shown in Fig. 3(b), shows strong optical confinement with a high Q factor of 1290 because large refractive index difference between the GeSn active layer and air prevents the leakage of optical fields. The temperature of an active area, however, is increased significantly to  $\sim 500$  K upon the current injection due to poor thermal dissipation in the suspended device geometry. As the increased temperature hinders optical emission in the active area due to heat-induced optical loss and also due to the reduced optical gain at an elevated temperature<sup>28</sup>, an optimized structure was envisioned to achieve both good optical confinement and thermal dissipation. Fig. 3(c) presents an optimized structure in which a GeSn active layer is laid down onto a  $\text{SiO}_2$  substrate. It is worth mentioning that the optimized structure can be fabricated using the GeSnOI substrate, which has recently been successfully demonstrated by several research groups<sup>11,25,26,29</sup>. The optimized structure shows the simultaneous achievement of good heat dissipation with slightly increased temperature of  $\sim 20$  K and superior optical confinement with a high Q factor of 1160. We believe that it is feasible to achieve lasing in the optimized structure.

## II. CONCLUSION

In summary, microbridge PIN GeSn LEDs were demonstrated and their operation performance was assessed using electrical and optical characterizations. It was found that the microbridge LED has power dissipation as low as 3 W and a small footprint of  $1,520 \mu\text{m}^2$ . The efficient thermal dissipation of the current design helped reduce the heat-induced optical losses and thus enhanced light emission. According to thermal and optical simulations, the microbridge design can be promising for lasing if a similar device was fabricated on GeSnOI substrate.

TABLE I. LED performance comparison

Device	Footprint area ( $\mu\text{m}^2$ )	Current Density ( $\text{A}/\text{cm}^2$ )	Bias (V)	Dissipated Power (W)	Temp. (K)
Ref <sup>16</sup>	7850	26	–	–	300
Ref <sup>17</sup>	8000	2000	0.2	400	300
Ref <sup>18</sup>	31400	191	0.9	18	300
Ref <sup>14</sup>	$10^6$	1.5	0.25	3.75	300
<b>This work</b>	1520	66	3	3	80
		143	5	10.8	300

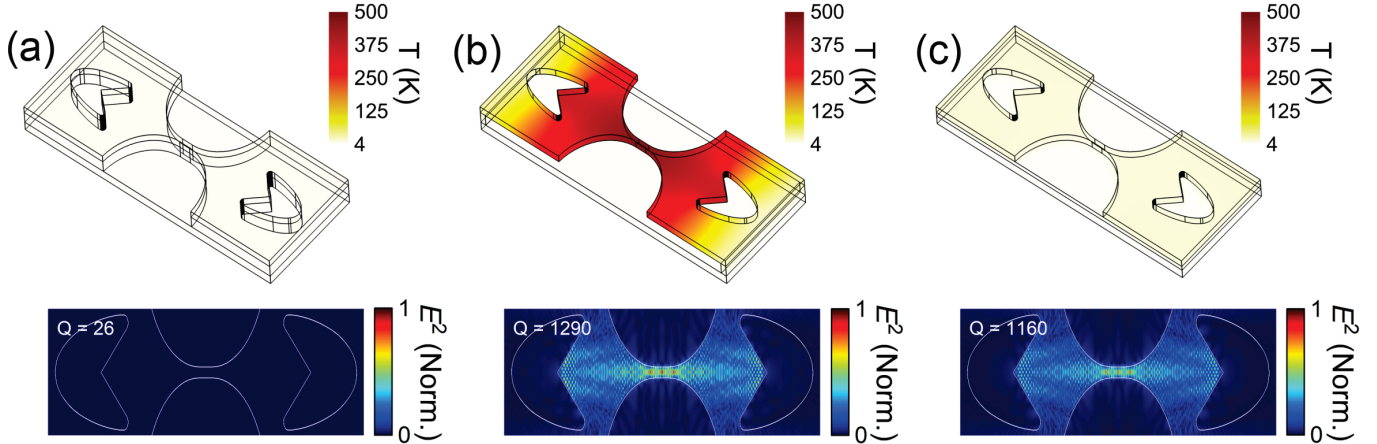


FIG. 3. Simulation for the thermal dissipation and optical confinement for the microbridge LED in three cases: (a) unreleased structure without under etch of Ge VS (current device). (b) Suspended structure with Ge VS under-etched. (c) Complete under etch of the Ge VS layer to fully release the PIN GeSn microbridge layer and place it on SiO<sub>2</sub> substrate.

**Acknowledgements.** The work carried out in Montréal was supported by Natural Science and Engineering Research Council of Canada (Discovery, SPG, and CRD Grants), Canada Research Chairs, Canada Foundation for Innovation, Mitacs, PRIMA Québec, and Defence Canada (Innovation for Defence Excellence and Security, IDEaS). The research performed at Nanyang Technological University was supported by Ministry of Education, Singapore, under grant AcRF TIER 1 2019-T1-002-050 (RG 148/19 (S)). The research of the project was also supported by Ministry of Education, Singapore, under grant AcRF TIER 2 (MOE2018-T2-2-011 (S)). This work was also supported by National Research Foundation of Singapore through the Competitive Research Program (NRF-CRP19-2017-01). This work was also supported by National Research Foundation of Singapore

through the NRF-ANR Joint Grant (NRF2018-NRF-ANR009 TIGER). This work was also supported by the iGrant of Singapore A\*STAR AME IRG (A2083c0053). The authors would like to acknowledge and thank the Nanyang NanoFabrication Centre (N2FC).

**Author information.** Mahmoud R. M. Atalla and Youngmin Kim have contributed equally to this work. Correspondence and requests for materials should be addressed to :  
 oussama.moutanabbir@polymtl.ca and  
 dnam@ntu.edu.sg

**Data availability.** The data that support the findings of this study are available from the corresponding author upon reasonable request.

<sup>1</sup> Soref, R. Silicon-based silicogermaniumtin heterostructure photonics. *Philosophical Transactions of the Royal Society A: Mathematical, Physical and Engineering Sciences* **372** (2014). URL <https://royalsocietypublishing.org/doi/10.1098/rsta.2013.0113>.

<sup>2</sup> Saito, S. *et al.* Group IV light sources to enable the convergence of photonics and electronics. *Frontiers in Materials* **1**, 15 (2014).

<sup>3</sup> Deen, M. J. & Basu, P. K. Silicon Photonics: Fundamentals and Devices. *Silicon Photonics: Fundamentals*

- and Devices 1–433 (2012). URL <https://onlinelibrary.wiley.com/doi/book/10.1002/9781119945161>.
- <sup>4</sup> Soref, R. The past, present, and future of silicon photonics. *IEEE Journal on Selected Topics in Quantum Electronics* **12**, 1678–1687 (2006).
  - <sup>5</sup> Liang, D. & Bowers, J. E. Recent progress in lasers on silicon. *Nature Photonics* **2010 4:8** **4**, 511–517 (2010). URL <https://www.nature.com/articles/nphoton.2010.167>.
  - <sup>6</sup> Zhou, Z., Yin, B. & Michel, J. On-chip light sources for silicon photonics. *Light: Science & Applications* **4**, e358–e358 (2015).
  - <sup>7</sup> Moutanabbir, O. *et al.* Monolithic infrared silicon photonics: The rise of (Si)GeSn semiconductors. *Applied Physics Letters* **118**, 110502 (2021). URL <https://aip.scitation.org/doi/abs/10.1063/5.0043511>.
  - <sup>8</sup> von den Driesch, N. *et al.* Direct Bandgap Group IV Epitaxy on Si for Laser Applications. *Chemistry of Materials* **27**, 4693–4702 (2015). URL <https://pubs.acs.org/doi/10.1021/acs.chemmater.5b01327>.
  - <sup>9</sup> Wirths, S. *et al.* Lasing in direct-bandgap gesn alloy grown on si. *Nature photonics* **9**, 88–92 (2015).
  - <sup>10</sup> Atalla, M. *et al.* All-Group IV Transferable Membrane Mid-Infrared Photodetectors. *Advanced Functional Materials* **31** (2021).
  - <sup>11</sup> Moutanabbir, O. *et al.* Optically pumped low-threshold microdisk lasers on a GeSn-on-insulator substrate with reduced defect density. *Photonics Research, Vol. 10, Issue 6, pp. 1332-1337* **10**, 1332–1337 (2022). URL <https://opg.optica.org/viewmedia.cfm?uri=prj-10-6-1332&seq=0&html=truehttps://opg.optica.org/abstract.cfm?uri=prj-10-6-1332https://opg.optica.org/prj/abstract.cfm?uri=prj-10-6-1332>.
  - <sup>12</sup> Buca, D. *et al.* Room Temperature Lasing in GeSn Microdisks Enabled by Strain Engineering. *Advanced Optical Materials* **10**, 2201024 (2022). URL <https://onlinelibrary.wiley.com/doi/full/10.1002/adom.202201024https://onlinelibrary.wiley.com/doi/abs/10.1002/adom.202201024https://onlinelibrary.wiley.com/doi/10.1002/adom.202201024>.
  - <sup>13</sup> Marzban, B. *et al.* Strain Engineered Electrically Pumped SiGeSn Microring Lasers on Si. *ACS Photonics* **10**, 217–224 (2022). URL <https://pubs.acs.org/doi/full/10.1021/acsp Photonics.2c01508>.
  - <sup>14</sup> Oehme, M. *et al.* Room-temperature electroluminescence from GeSn light-emitting pin diodes on Si. *IEEE Photonics Technology Letters* **23**, 1751–1753 (2011).
  - <sup>15</sup> Tseng, H. H. *et al.* Mid-infrared electroluminescence from a Ge/Ge<sub>0.922</sub>Sn<sub>0.078</sub>/Ge double heterostructure p-i-n diode on a Si substrate. *Applied Physics Letters* **102**, 182106 (2013). URL <https://aip.scitation.org/doi/abs/10.1063/1.4804675>.
  - <sup>16</sup> Gupta, J. P., Bhargava, N., Kim, S., Adam, T. & Kolodzey, J. Infrared electroluminescence from GeSn heterojunction diodes grown by molecular beam epitaxy. *Applied Physics Letters* **102**, 251117 (2013). URL <https://aip.scitation.org/doi/abs/10.1063/1.4812747>.
  - <sup>17</sup> Gallagher, J. D. *et al.* Electroluminescence from GeSn heterostructure pin diodes at the indirect to direct transition. *Applied Physics Letters* **106**, 091103 (2015). URL <https://aip.scitation.org/doi/abs/10.1063/1.4913688>.
  - <sup>18</sup> Stange, D. *et al.* Short-wave infrared LEDs from GeSn/SiGeSn multiple quantum wells. *Optica* **4**, 185 (2017).
  - <sup>19</sup> Peng, L. *et al.* Horizontal GeSn/Ge multi-quantum-well ridge waveguide LEDs on silicon substrates. *Photonics Research* **8**, 899 (2020). URL <https://opg.optica.org/prj/abstract.cfm?uri=prj-8-6-899https://opg.optica.org/abstract.cfm?URI=prj-8-6-899>.
  - <sup>20</sup> Huang, B. J. *et al.* Electrically Injected GeSn Vertical-Cavity Surface Emitters on Silicon-on-Insulator Platforms. *ACS Photonics* **6**, 1931–1938 (2019). URL <https://pubs.acs.org/doi/full/10.1021/acsp Photonics.8b01678>.
  - <sup>21</sup> Armand Pilon, F. *et al.* Lasing in strained germanium microbridges. *Nature communications* **10**, 2724 (2019).
  - <sup>22</sup> Son, B., Lin, Y., Lee, K. H., Chen, Q. & Tan, C. S. Dark current analysis of germanium-on-insulator vertical p-i-n photodetectors with varying threading dislocation density. *Journal of Applied Physics* **127**, 203105 (2020).
  - <sup>23</sup> Dong, Y. *et al.* Two-micron-wavelength germanium-tin photodiodes with low dark current and gigahertz bandwidth. *Optics Express* **25**, 15818 (2017). URL <https://doi.org/10.1364/OE.25.015818>.
  - <sup>24</sup> Atalla, M. R. M., Assali, S., Koelling, S., Attiaoui, A. & Moutanabbir, O. Dark current in monolithic extended-SWIR GeSn PIN photodetectors. *Applied Physics Letters* **122**, 031103 (2023). URL <https://aip.scitation.org/doi/abs/10.1063/5.0124720>.
  - <sup>25</sup> Burt, D. *et al.* Strain-relaxed GeSn-on-insulator (GeSnOI) microdisks. *Optics Express, Vol. 29, Issue 18, pp. 28959-28967* **29**, 28959–28967 (2021). URL <https://opg.optica.org/viewmedia.cfm?uri=oe-29-18-28959&seq=0&html=truehttps://opg.optica.org/abstract.cfm?uri=oe-29-18-28959https://opg.optica.org/oe/abstract.cfm?uri=oe-29-18-28959>.
  - <sup>26</sup> Joo, H. J. *et al.* 1D photonic crystal direct bandgap GeSn-on-insulator laser. *Applied Physics Letters* **119**, 201101 (2021). URL <https://aip.scitation.org/doi/abs/10.1063/5.0066935>.
  - <sup>27</sup> Gupta, S. *et al.* Highly selective dry etching of germanium over germanium-tin (Ge<sub>1-x</sub>Sn<sub>x</sub>): A novel route for Ge<sub>1-x</sub>Sn<sub>x</sub> nanostructure fabrication. *Nano Letters* **13**, 3783–3790 (2013). URL <https://pubs.acs.org/doi/full/10.1021/nl14017286>.
  - <sup>28</sup> Kim, Y. *et al.* Enhanced GeSn Microdisk Lasers Directly Released on Si. *Advanced Optical Materials* **10**, 2101213 (2022). URL <https://onlinelibrary.wiley.com/doi/full/10.1002/adom.202101213https://onlinelibrary.wiley.com/doi/abs/10.1002/adom.202101213https://onlinelibrary.wiley.com/doi/10.1002/adom.202101213https://onlinelibrary.wiley.com/doi/10.1002/adom.202101213>.
  - <sup>29</sup> Wang, B. *et al.* GeSnOI mid-infrared laser technology. *Light Science & Applications* **10**, 1–13 (2021). URL <https://www.nature.com/articles/s41377-021-00675-7>.